WSRC-MS-98-00857

Design of a Carousel Process for Removing Cesium from SRS Waste Using Crystalline Silicotitanate Ion Exchanger

RECORDS ADMINISTRATION
R0097852

by
D. D. Walker
Westinghouse Savannah River Company
Savannah River Site
Aiken, South Carolina 29808

B. J. Hritzko

N. -H. Linda Wang

DOE Contract No. **DE-AC09-96SR18500**

This paper was prepared in connection with work done under the above contract number with the U. S. Department of Energy. By acceptance of this paper, the publisher and/or recipient acknowledges the U. S. Government's right to retain a nonexclusive, royalty-free license in and to any copyright covering this paper, along with the right to reproduce and to authorize others to reproduce all or part of the copyrighted paper.

DISCLAIMER

This report was prepared as an account of work sponsored by an agency of the United States Government. Neither the United States Government nor any agency thereof, nor any of their employees, makes any warranty, express or implied, or assumes any legal liability or responsibility for the accuracy, completeness, or usefulness of any information, apparatus, product, or process disclosed, or represents that its use would not infringe privately owned rights. Reference herein to any specific commercial product, process, or service by trade name, trademark, manufacturer, or otherwise does not necessarily constitute or imply its endorsement, recommendation, or favoring by the United States Government or any agency thereof. The views and opinions of authors expressed herein do not necessarily state or reflect those of the United States Government or any agency thereof.

This report has been reproduced directly from the best available copy.

Available to DOE and DOE contractors from the Office of Scientific and Technical Information, P. O. Box 62, Oak Ridge, TN 37831; prices available from (423) 576-8401.

Available to the public from the National Technical Information Service, U. S. Department of Commerce, 5285 Port Royal Road, Springfield, VA 22161.

WSRC-MS-98-00857

KEYWORDS: Salt processing
Ion Exchange
High level waste

RETENTION PERIOD: Until Superceded or obsolete

Design of a Carousel Process for Removing Cesium from SRS Waste Using Crystalline Silicotitanate Ion Exchanger

Benjamin J. Hritzko and N.-H. Linda Wang
School of Chemical Engineering, Purdue University, West Lafayette, IN 47907-1283

D. Douglas Walker
Westinghouse Savannah River Company, Aiken, SC 29808

Abstract

Designs of a three-column carousel process based on crystalline silicotitanate (CST) ion exchanger have been developed for removing radioactive $^{137}Cs^+$ from Savannah River Site's (SRS) nuclear wastes. A multicomponent ion exchange equilibrium model (Zheng et al., 1997) from Texas A&M University, which is based on batch data obtained from CST powder, is used to generate cesium loading data at different cesium concentrations for various types of SRS wastes. These loading data are fit to the Langmuir equation to obtain effective single-component cesium isotherm parameters. The predictions are in reasonable agreement with batch test data obtained from CST powder, an early CST pellet batch (38B), and a later batch (IE911) using two SRS waste simulants. The ratios between experimental cesium distribution coefficients and predicted values are between 0.56 and 1.0. The variation appears to be due to inadequate equilibration time in some of the batches. Mass transfer parameters are estimated by analyzing column data of a simulated SRS waste and Melton Valley Storage Tank W29 (MVST-W29) waste. The intraparticle diffusivity estimated for the two wastes can be well correlated by means of the Stokes-Einstein equation.

Simulations are performed to determine the length of the mass transfer zone for given feed compositions, Cs^+ concentrations, and linear velocities. In order to ensure high column utilization during both the transient and cyclic steady state periods, the length of a single segment in the carousel process is chosen to be the mass transfer zone length after the concentration wave achieves a constant pattern. Analysis of the dimensionless groups in the differential mass balance equations reveals that the normalized mass transfer zone length is linearly proportional to the particle Peclet number. The proportionality constant is a function of the waste composition and the Cs^+ concentration in the waste. The higher the effective Cs^+ capacity and the higher the Cs^+ concentration, the smaller the proportionality constant. This dimensionless group analysis allows one to easily adjust designs for variations in particle size, linear velocity, and intraparticle diffusivity.

Introduction

Over 100 million gallons of radioactive waste, generated by nuclear reactors and weapon production plants, is now in underground storage tanks (USTs) at Department of Energy (DOE) sites in Hanford, Savannah River, Oak Ridge, Idaho, and Fernald (McGinnis et al., 1995). The cost for treating this waste using current technologies is estimated at 100 billion dollars (McGinnis et al., 1995). After the initial treatment, the waste in its final form is enclosed in borosilicate glass for permanent storage.

Several different approaches are currently under investigation for treating the supernatant before it is placed in long-term storage (McGinnis et al., 1995). The present study is focused on CST ion exchange for treatment of Savannah River Site (SRS) wastes. CST has a high affinity for the major radioactive contaminant $^{137}Cs^+$. Since the affinity is high, a large amount of $^{137}Cs^+$ can be confined within a small volume of saturated CST particles. Since the cost of making glass canisters is expected to be quite high, it is important to utilize the CST exchanger as much as possible. A continuous carousel process with three packed columns in series (Figure 1) is proposed. The carousel design allows the cesium level in the decontaminated waste to be below the required levels (less than 1.3×10^{-3} mg/L Cs^+) and almost full utilization of the adsorbent (Ernest et al., 1997).

CST ion exchanger was developed at Texas A\&M University (TAMU) in a powder form (Anthony et al., 1993; Anthony et al., 1994) and was engineered into a pellet form by UOP. The pellet form is the CST powder mixed with an inert binder. This binder makes CST feasible for column applications, but it is expected to give the pellets a lower effective capacity per unit weight than the powder (McCabe, 1995; McCabe, 1997). Zheng et al. (1997) at TAMU developed a detailed multicomponent ion exchange model that describes the uptake of Cs^+ on CST powder in the presence of competing ions. They validated the model via batch experiments conducted in ORNL, NCAW and other waste simulants in which Cs^+ loading on CST powder was measured (Zheng et al., 1997).

In this work, the equilibrium uptakes of Cs^+ on CST powder predicted from the TAMU model have been fit to a single-component Langmuir isotherm for six different SRS waste compositions. The batch test data obtained for CST pellets (38B and IE911) can be explained by a dilution factor of 0.56 to 1.0. This approach yields effective Cs^+ isotherms, which are needed in a dynamic column model for the carousel design.

Mass transfer parameters are estimated by analyzing breakthrough data of an SRS waste simulant, as well as data from Cesium Removal Demonstration (CsRD) column experiments and CsRD support column experiments from Oak Ridge National Laboratory (ORNL). The CsRD experiments were performed on CST pellets from the same lot and with the same feed (Melton Valley Storage Tank W29, or MVST-W29) over a wide range of linear superficial velocities (0.3 to 10.8 cm/min). Porous column model simulations are compared to the column data and the effective intraparticle diffusivities (D_p) are determined for the SRS waste simulant and the MVST-W29 waste. The Stokes-Einstein equation is shown to correlate the values of D_p for the two different wastes, based on the viscosities of the wastes. For both feeds the model yields a close fit to the column data. The ORNL 50 percent breakthrough times can be well predicted using the TAMU model with a dilution factor from 0.56 to 0.66. The SRS column data can be well explained by the TAMU model with a dilution factor of 1.0.

The model and mass transfer parameters are used in simulations to obtain carousel designs for treating large-scale SRS waste. The length of the mass transfer zone determines the column length requirement for the segments in a carousel process. The mass transfer zone is defined as the length of column required to contain the Cs^+ concentration wave from 90 percent of the feed concentration to 1.3×10^{-3} mg/L. An analysis of the dimensionless groups in the model has shown that the mass transfer zone length (normalized by the particle radius) depends only on the particle Peclet number. The proportionality constant in this relationship is a function of the Cs^+ concentration and the effective Cs^+ isotherm parameters, which depend on the waste compositions. Using this linear relation, one can easily determine the carousel column size at a given linear velocity, particle size, and intraparticle diffusivity.

This study establishes a model-based design approach that is efficient and requires relatively few experiments. This approach gives carousel designs with high column utilization both during startup and at cyclic steady state. This method can be applied to design carousel ion exchange processes for other complex wastes.

Simulation Models, Parameters, and Assumptions

The mathematical model utilized in the simulations is a porous model which takes into account competitive adsorption, bulk convection, axial dispersion, film mass transfer, and pore diffusion. Since surface diffusion effects are not evident from the available data, the pore diffusion model is used in this analysis. The numerical solutions of the governing equations and boundary conditions are performed by the VERSE simulation package (Berninger et al., 1997; Whitley, 1990). This model has been validated in many previous studies (Ernest et al., 1997; Koh et al., 1998; Ma et al., 1996). The pore diffusion model assumes uniform spherical adsorbent particles, plug flow with constant linear velocity, local equilibrium within the adsorbent and constant diffusivities.

Pore diffusion model

In the pore diffusion model, the material balance in the mobile phase is given by

$$\frac{\partial C}{\partial t} = E_b \frac{\partial^2 C}{\partial z^2} - u_0 \frac{\partial C}{\partial z} - \frac{3k_f(1-\varepsilon_b)}{R_p \varepsilon_b}(C - C_{p,r=R_p}) \tag{1}$$

$$z = 0, \quad E_b \frac{\partial C}{\partial z} = u_0 (C(t,0) - C_0)$$

$$z = L, \quad \frac{\partial C}{\partial z} = 0$$

$$t = 0, \quad C = C(0,z)$$

where C is the mobile phase concentration (mg/mL), t is time (min), E_b is the axial dispersion coefficient (cm^2/min), z is the axial distance along the column (cm), u_0 is the mobile phase velocity (cm/min), k_f is the film mass transfer coefficient (cm/min), R_p is the particle radius (cm), and $C_{p,r=Rp}$ is the particle phase solute concentration at the surface (mg/mL). In the pore phase, the material balance equation is

$$\left(\varepsilon_p + (1-\varepsilon_p)\frac{\partial q}{\partial C_p}\right)\frac{\partial C_p}{\partial t} = \varepsilon_p \frac{D_p}{r^2}\frac{\partial}{\partial r}\left(r^2 \frac{\partial C_p}{\partial r}\right) \tag{2}$$

$$r = 0, \quad \frac{\partial C_p}{\partial r} = 0$$

$$r = R_p, \quad e_p D_p \frac{\partial C_p}{\partial r} = k_f R_p (C - C_{p,r=R_p})$$

$$t = 0, \quad C_p = C_p(0,r)$$

where C_p is the pore-phase concentration (mg/mL), q is the solid-phase concentration (mg/mL S.V.), r is the distance in the radial direction (cm), and D_p is the intraparticle diffusivity (cm^2/min).

Eqs. 1 and 2 and their boundary conditions can be rewritten as follows in terms of the dimensionless quantities listed in Table 1.

$$\frac{\partial C}{\partial \theta} = \frac{1}{\mathrm{Pe}_b}\frac{\partial^2 C}{\partial x^2} - \frac{\partial C}{\partial x} - 3L_c^* \phi_b k_f^* (C - C_{p,\xi=1}) \tag{3}$$

$$x = 0, \quad \frac{\partial C}{\partial x} = Pe_b (C - C_0(\theta))$$

$$x = 1, \quad \frac{\partial C}{\partial x} = 0$$

$$\theta = 0, \quad C = C(0,x)$$

$$\left(1+\phi_p \frac{\partial q}{\partial C_p}\right)\frac{\partial C_p}{\partial \theta} = L_c^* \frac{1}{\mathrm{Pe}_p}\frac{1}{\xi^2}\frac{\partial}{\partial \xi}\left(\xi^2 \frac{\partial C_p}{\partial \xi}\right) \tag{4}$$

$$\xi = 0, \quad \frac{\partial C_p}{\partial \xi} = 0$$

$$\xi = 1, \quad \frac{\partial C_p}{\partial \xi} = \frac{1}{1+\phi_p} Pe_p k_f^* (C - C_p)$$

$$\theta = 0, \quad C_p = C_p(0,\xi)$$

Effective Cs^+ isotherm approach for complex wastes

Figure 2 shows effective Cs^+/CST isotherms based on TAMU model predictions for the various SRS wastes. The compositions of the SRS wastes are listed in Table 2. Figure 3 shows the TAMU model predictions for the SRS standard simulant and the batch test data for CST powder (McCabe, 1995) and CST pellets (McCabe, 1997). The experimental data are in reasonable agreement with the model predictions. The waste is a complex multicomponent mixture and the TAMU model (Zheng et al., 1997) is able to predict to within ± 20 percent the effective adsorption capacity of Cs^+ at various feed Cs^+ concentrations for the SRS standard simulant. In the simulations, a simple Langmuir isotherm is chosen to describe the equilibrium uptake of Cs^+ on CST. TAMU model isotherms are fit to individual Langmuir isotherms. For the W29 waste, it is necessary to multiply the Langmuir coefficient *a* by a dilution factor. This factor has been justified in two separate instances. Figure 3a shows experimental batch data for powdered CST (DG-112) and batch data for the engineered form (38B), both in SRS standard simulant. The maximum capacity (at high concentration) of the engineered form is 56 percent of that of the powdered form. At low concentrations, the dilution factor is between 0.7 and 1.0. The solid line shows that the TAMU model can predict Cs^+ uptake on the powdered CST reasonably well. The uptake of Cs^+ on the engineered form is in reasonable agreement with the TAMU model prediction multiplied by dilution factors of 0.56 and 0.7 (dashed lines in Figure 3). This lower dilution factor for the pellet at high Cs^+ concentration could be due to nonequilibrium data, since the samples in the batch tests were taken at 48 hours. This hypothesis is supported by batch test data obtained by Hunt et al. (1998) shown in Figure 3b. The batch data collected at 24 and 72 hours are not at equilibrium, evident from time-varying concentration. For these large particles, the equilibration time should be 168 hours or more. In a second case, shown in Figure 4, the TAMU model for Cs^+ uptake on powdered CST in the MVST-29 waste is denoted by a solid line. The two dotted lines show the best-fit Langmuir isotherms to column data performed on IE911 with the MVST-W29 waste. All of the column data are well predicted by isotherm parameters within this range. The maximum capacities determined from these two isotherms (on engineered CST) are 56 percent and 66 percent of that of the powdered form CST. This low dilution factor could be due to the following factors: a combination of the presence of an inert binder, TAMU model inaccuracy, or the presence of competing ions in the real waste (such as Zn, Pb, and Ba) that are not considered in the TAMU model. Table 3 lists the Langmuir isotherm parameters for W29 and various SRS wastes.

Mass transfer parameters

Melton Valley Storage Tank W29 Column Tests. The Brownian diffusivity for W29 is taken from the work of Ernest et al. (1997). The Brownian diffusivity for the SRS wastes is assumed to be 73 percent of that for W29, according to the Stokes-Einstein equation (Eq. 5 below). The film mass transfer coefficient, k_f, is calculated from the correlation by Wilson and Geankoplis (1966) and the axial dispersion coefficient, E_b, is calculated from the correlation by Chung and Wen (1968). These parameters are used to analyze ORNL CST small-scale (10 mL) column data (Lee et al., 1997) and large-scale (38 L) column data (J. F. Walker et al., 1998). Simulation results are compared to the experimental data. It is found that the breakthrough times are well predicted when the isotherm parameters for W29 from the TAMU model are adjusted by a factor of 0.56 to 0.66, indicating the effective Cs^+ isotherm approach is

successful in predicting Cs breakthrough in a complex mixture. The intraparticle diffusivity, D_p, is then fit to the small-scale frontal data. Figures 5a-c show the comparison of experimental data to simulation results for small scale CsRD support runs by D. D. Lee. These parameters were then used to predict the large-scale frontal data, and it was found that the large-scale breakthrough curves were slightly more spread than predicted. Figures 6 and 7 show the comparison of experiment to simulation for large scale CsRD column experiments. This indicates that dispersion in the large columns is greater than in small columns, perhaps as a result of different packing procedures.

Westinghouse Savannah River Company Column Tests. Since MVST waste has a viscosity of 1.6 cp and SRS waste has a viscosity of 2.2 cp, the value of D_p determined from the CsRD column tests is not valid for designing columns to handle SRS waste. According to the Stokes-Einstein equation, the diffusivity is related to the solution viscosity:

$$D = \frac{k_B T}{6 \pi \mu R_0} \tag{5}$$

where D is the diffusivity, k_B is Boltzmann's constant, T is absolute temperature, μ is the viscosity, and R_0 is the solute radius. The value of the diffusivity is inversely proportional to the fluid viscosity, so that the intraparticle diffusivity for SRS wastes is estimated to be

$$1.0 \times 10^{-4} \left(\frac{1.6}{2.2} \right) = 7.3 \times 10^{-5} \text{ cm}^2 / \text{min} \tag{6}$$

Preliminary column data are obtained for SRS average waste on CST pellets (D. D. Walker et al., 1998). The column experiments can be well predicted assuming a dilution factor of 1.0 and a D_p of 7.3×10^{-5} cm^2/min (Eq. 6). Figure 8 shows column effluent histories for three runs in a laboratory-scale column (17.7 mL) at three different linear superficial velocities (u_s = 0.27, 0.98, and 4.1 cm/min). Flow rate and Cs^+ feed concentration are taken into account in the model. The positions and shapes of the breakthrough curves are well predicted by the model. The isotherm parameters, mass transfer model and the correlation of D_p using the Stokes-Einstein equation appear to be valid.

Column parameters

The particle size, interparticle void fraction (ε_b), and intraparticle void fraction (ε_p) were based on the known densities of the CST particles (Anthony, 1998). In the mathematical model, it is assumed that all the particles are spherical and of uniform size (375 μm in diameter). Table 4 lists the simulation parameters. These mass transfer and system parameters have been employed to design large-scale carousel processes for treating SRS wastes.

Design Approach

Determination of constant-pattern mass transfer zone length

The first step in the design is to determine the mass transfer zone length, which is a function of the isotherm parameters, Cs^+ feed concentrations, mass transfer parameters, and linear velocity. The mass transfer zone length is examined at two different flow rates—15 and 25 gpm, which correspond to two different superficial velocities (4.9 and 8.1 cm/min, respectively). Since the isotherm is nonlinear at the concentration level in the SRS waste (Figure 2), the concentration waves eventually develop into a constant pattern. A sufficiently long column (66 ft) is chosen in this simulation so that the waves can reach a constant pattern. Figures 9a-b demonstrate the mass transfer zone length determination. The length of the mass transfer zone is determined from the concentration profile where the local concentration decreases from 90 percent of the feed concentration to 1.3×10^{-3} mg/L. The feed compositions are listed in Table 2. Notice that the concentration of Cs^+ varies from waste to waste. For this specification, the percent saturation in the lead column is much higher than 90 percent (the target for large-scale applications). Clearly, the mass transfer zone length, L_{MTZ}, increases on increasing column length and reaches a maximum value when a constant pattern develops.

If one chooses the constant pattern L_{MTZ}, the carousel design is straightforward. A three-segment carousel will have a total length of 3 L_{MTZ}. The choice of constant pattern L_{MTZ} to be the column length will ensure that when the carousel operation reaches cyclic steady state, the percent sorbent utilization in the lead column (saturation zone) will satisfy the 90 percent or higher utilization desired. VERSE simulations confirm this. An example is shown in Figure 11.

Case 1: Carousel designs for a fixed column diameter

For practical applications, a column diameter of about 4 ft and a segment length of 16 ft or smaller are desired. Table 5 lists the column length requirements for the six SRS feeds when the column diameter is fixed at 4 ft. For each isotherm, we have determined the mass transfer zone length for two flow rates (15 gpm and 25 gpm).

Dimensionless group analysis

By examining the differential mass balance equations and boundary conditions, Eqs. 3 and 4, one expects that the concentration profile or dimensionless mass transfer zone length, L_{MTZ}^*, at constant pattern is a function of the dimensionless groups of the equations (L_c^*, k_f^*, ϕ_b, ϕ_p, Pe_p, and Pe_b), the isotherm parameters, and the feed Cs^+ concentration. For a sufficiently long column ($L_c/R_p > 1000$) at a relatively high linear velocity $u_0 > 0.25$ cm/min), L_{MTZ}^* is controlled by intraparticle diffusion. Therefore, L_{MTZ}^* is only a function of Pe_p for a given waste. This relationship can be summarized as:

$$L_{MTZ}^* \propto Pe_p \tag{7}$$

where

$$L_{MTZ}^* \equiv \frac{L_{MTZ}}{R_p} \tag{8}$$

is the dimensionless mass transfer zone length. Eq. 7 states that the length of the mass transfer zone is directly proportional to the linear velocity and the square of the particle radius and that it is inversely proportional to the intraparticle diffusivity. Figure 10 shows the relationship between the dimensionless mass transfer zone and the Peclet number. It should be pointed out that the slope of the line in each case depends on both the waste type and the cesium concentration. If the waste composition remains the same as those in Table 2, Figure 10 provides a convenient estimate of L_{MTZ} (or carousel size) when R_p, D_p, or u_0 is varied.

Two important trends are apparent from Figure 10. First, for a given Cs^+ concentration, L_{MTZ}^* decreases with increasing Langmuir a value. One can see in Figure 10 that for the bounding cases, in which the Cs^+ concentration is 0.0007 M, L_{MTZ}^* is highest for the "High NO_3-b" case and lowest for the "High OH-b" case for all values of Pe_p. Recall from Table 3 that the "High NO_3-b" case has the lowest Langmuir a value and the "High OH-b" case has the highest a value among the three bounding cases. Second, for a given isotherm, a higher Cs^+ concentration leads to a lower L_{MTZ}^*. This can be seen in the "High NO_3-b" case, which has the lowest Langmuir a value among the six wastes but has a lower L_{MTZ}^* than the nominal cases because its Cs^+ concentration is 1.9 times higher than the "High OH" case and five times higher than the "Average" and "High NO_3" cases.

Case 2: Carousel designs for a fixed column length

For the six different types of SRS wastes, the segment lengths (or L_{MTZ}) are less than 16 ft with two exceptions, the 25 gpm cases for the "Average Waste" and the "High NO_3 Waste" (Table 5). For these two cases and the other wastes, we investigate the designs with a fixed segment length of 16 ft and a diameter that is either larger or smaller than 4 ft. The results are reported in Table 6. When the segment length is fixed at 16 ft, this implies that L_{MTZ} is fixed at 16 ft for all the different feeds, whereas the linear velocity u_0 is varied to achieve this goal. The u_0 values are determined by finding the Peclet number that gives L_{MTZ} = 16 ft. Column diameters that can handle 15 gpm and 25 gpm are calculated according to a given u_0. Notice that for a given feed, the linear velocity is the same for 15 and 25 gpm. A change in the column diameter allows for a change in the volumetric flow rate.

As clearly shown in Table 5, the L_{MTZ} for 4-ft diameter columns for some cases are less than 16 ft. Therefore the column diameter in Table 6 can be reduced to below 4 ft and a higher u_0 can be used. In contrast, for the cases in Table 5 where the L_{MTZ} are longer than 16 ft, a lower u_0 must be used to confine the mass transfer zone to 16 ft, and column diameters must be increased to above 4 ft to accommodate 15 gpm and 25 gpm feed flow rates.

Transient behavior of proposed carousel processes

For the "Average" waste, 15 gpm throughput require a three-column carousel which is 4 ft in diameter and 11.3 ft in segment length, while 25 gpm throughput requires a carousel which is 4.3 ft in diameter and 16 ft in segment length. These two cases are compared in Table 7. Actual carousel simulations are carried out to check the percent column saturation during the transient period and at cyclic steady state. In the carousel process simulations, the port switching occurs when the outlet concentration of the second column reaches 1.3×10^{-3} mg/L. At this time, the first column is taken off-line, the feed is introduced into the second column, and a fresh column introduced at the end of the train (as a guard column). Figure 11 shows the simulated concentration histories at the outlet of each column for two carousel processes, one operated at 15 gpm and the other at 25 gpm. Notice that in both cases the outlet concentration of column 2 reaches the specified value of 1.3×10^{-3} mg/L at the port switching time. The outlet concentration of column 3 (the guard column) is too low to be seen in this figure. Figure 11 also shows that cyclic steady state is established after about three switching periods. The utilization of the lead column is about 99.8 percent before cyclic steady state is established and 99.2 percent at cyclic steady state. This result proves that by choosing the constant pattern L_{MTZ}, one can ensure that percent utilization is high during the startup and after cyclic steady state is established.

Design Alternatives

There are many alternative carousel designs that can meet SRS waste treatment requirements. The sizes of the carousel columns in Tables 5 and 6 are estimated based on a fixed diameter for Case 1 and a fixed segment length of 16 ft for Case 2 and the following assumptions: (1) The effective Cs^+ isotherms of the wastes can be predicted by using the TAMU model with a dilution factor of 1.0. (2) The D_p value is 7.3×10^{-5} cm^2/min for all wastes. (3) The L_{MTZ} is defined as the length in which C decreases from $0.9C_0$ to 1.3×10^{-3} mg/L. This definition gives a percent utilization of 99.8 during the startup and 99.2 percent at cyclic steady state. One can choose a shorter L_{MTZ} if a lower percent utilization of the lead column is desired or the level of Cs^+ in the effluent of column 2 can be higher than 1.3×10^{-3} mg/L. (4) The current design assumes three columns: the lead column is for saturation; the second column is to contain

the mass transfer zone; and the third column is a guard column. Each column length is the same as the mass transfer zone length.

Alternatively, the mass transfer zone can be spread among two columns, thus halving the size of the lead column and the guard column in the process. The saturation zone and the guard zone decrease in length, while the mass transfer zone remains fixed, leading to a shorter overall bed length. Table 8 compares the performances of carousel processes with three, four, five, and six column segments. One can see that there is a 50 percent gain in the throughput per bed volume and a 33 percent decrease in the bed length on increasing the number of segments from three to four. However, there is also a 50 percent smaller guard column and one more valve. These factors need to be taken into account in future cost analyses and process optimization studies.

Conclusions

A model-based approach has been developed to design a CST carousel ion exchange process for removing cesium from Savannah River Site wastes. Batch equilibrium data were correlated using a detailed ion exchange model for CST powder (TAMU model). The model predictions were then fit to the Langmuir equation to obtain effective cesium isotherms for six model SRS waste compositions. For CST pellets in SRS standard simulant, a dilution factor from 0.56 to 1.0 is needed to fit the isotherm data. For W29 waste, a dilution factor of 0.56 to 0.66 is needed to fit the column data. However for the "Average" SRS simulant only, a dilution of 1.0 can explain the column data at three linear velocities. It appears that either the inert binder has no effect on the Cs^+ capacity or the TAMU model underestimates the Cs^+ loading in this waste simulant. This effective cesium isotherm approach was validated using the data from both small-scale and large-scale column tests at ORNL and small-scale column data for the "Average" SRS waste simulant. Axial dispersion and film mass transfer coefficients were calculated from well-known correlations, and the intraparticle diffusivity was determined by fitting porous model predictions to ORNL and SRS column data. These mass transfer parameters were validated over a wide range of linear velocities for the W29 wastes and the SRS simulant. The intraparticle diffusivities for the two wastes can be well correlated by the Stokes-Einstein equation.

In the design of the carousel process, the length of a single column segment is determined from the length of the mass transfer zone at a given linear velocity. The mass transfer zone is defined as the length of column required to contain the Cs^+ concentration band from $C = 0.9C_0$ to $C = 1.3 \times 10^{-3}$ mg/L after a constant pattern wave is developed. An analysis of the dimensionless groups in the differential mass balance equations reveals that the normalized mass transfer zone length is proportional to the particle Peclet number. The proportionality constant is a function of the waste composition and the Cs^+ concentration. For a given waste type, a higher Cs^+ concentration leads to a shorter mass transfer zone. For a given concentration, a higher Langmuir a value also yields a shorter mass transfer zone. For a given composition, modifications of a given design can be easily made by the use of this simple linear relation.

This study shows that the estimated carousel sizes are most sensitive to the effective cesium isotherms and the intraparticle diffusivities. The bed void fraction also has a direct impact on the size estimates. These key parameters should be confirmed by batch and column tests using actual SRS wastes before implementing the proposed designs for large-scale separation.

Acknowledgment

The authors wish to thank W. Tamosaitis and C. P. McGinnis for initiating this project; S. Beck and J. Carter for providing background information; R. Jacobs for calculating Cs^+ isotherms from the TAMU model; R. Anthony for providing the TAMU model as well as many system parameters; D. McCabe for providing SRS simulant batch data; D. D. Lee and P. Taylor for providing W29 column data; and R. D. Hunt, K. K. Anderson, and J. L. Collins for providing the batch test data on the "Average" SRS waste simulant.

Notation

a = Langmuir coefficient, mg/mL B.V.
b = Langmuir coefficient, mL/mg
C = bulk-phase solute concentration, mg/mL
C_p = pore-phase solute concentration, mg/mL
C_0 = column inlet solute concentration, mg/mL
D = diffusivity, cm^2/min
D_p = intraparticle diffusivity, cm^2/min
D^∞ = Brownian diffusivity, cm^2/min
E_b = axial dispersion coefficient, cm^2/min
F = volumetric flow rate, gpm or mL/min
I. D. = column inner diameter, ft
k_B = Boltzmann's constant, 4.97×10^{-13} g·cm^2/K·min^2
k_f= film mass transfer coefficient, cm/min
L_c = column length, cm or ft
q = solid-phase solute concentration, mg/mL S.V.
r = radial distance from center of adsorbent particle, cm
R_0 = solute radius, cm
R_p = adsorbent particle radius, cm or μm
t = time, min
T = absolute temperature, K
TPBV = throughput per bed volume, gpm/ft^3
u_0 = linear interstitial velocity, cm/min
u_s = linear superficial velocity, cm/min
V_c = column volume, mL or L
z = axial distance, cm

Greek letters
ε_b = bed void fraction, dimensionless
ε_p = intraparticle void fraction, dimensionless
μ = solution viscosity, g/cm·min

Dimensionless variables
$k_f = k_f/u_0$ (film mass transfer number)
$L_c^* = L_c/R_p$ (dimensionless column length)
$L_{MTZ}^* = L_{MTZ} / R_p$ (dimensionless mass transfer zone length)
$Pe_b = u_0 L_c / E_b$ (bulk Peclet number)
$Pe_p = u_0 R_p / \varepsilon_p D_p$ (particle Peclet number)
$x = z/L_c$ (dimensionless axial position)
$\theta = t\, u_0/L_c$ (dimensionless time)
$\xi = r/R_p$ (dimensionless radial position)
$\phi_b = (1-\varepsilon_b)/ \varepsilon_b$ (particle/bulk phase ratio)
$\phi_p = (1-\varepsilon_p)/ \varepsilon_p$ (solid/pore phase ratio)

Literature Cited

Anthony, R. G., R. G. Dosch, D. Gu, and C. V. Philip, "Use of Silicotitanates for Removing Cesium and Strontium from Defense Waste," *Ind. Eng. Chem. Res.*, **33**, 2702 (1994).

Anthony, R. G., C. V. Philip, and R. G. Dosch, "Selective Adsorption and Ion Exchange of Metal Cations and Anions with Silico-Titanates and Layered Titanates," *Waste Manage. (N.Y.)*, **13**, 503 (1993).

Anthony, R. G., Texas A&M University, personal communication (1998).

Berninger, J. A., R. D. Whitley, and N.-H. L. Wang, "A Versatile Model for Simulation of Reaction and Nonequilibrium Dynamics in Multicomponent Fixed-Bed Adsorption Processes," *Comp. Chem. Eng.*, **15**, 749 (1991).

Chung, S. F., and C. Y. Wen, "Longitudinal Dispersion of Liquid Flowing Through Fixed and Fluidized Beds," *AIChE J.*, **14**, 857 (1968).

Ernest, Jr., M. V., J. P. Bibler, R. D. Whitley, and N.-H. L. Wang, "Development of a Carousel Ion Exchange Process for Removal of Cesium-137 from Alkaline Nuclear Waste," *Ind. Eng. Chem. Res.*, **36**, 275 (1997).

Hunt, R. D., K. K. Anderson, and D. D. Lee, "Batch Tests with IONSIV IE-911 and a Simulant of the Savannah River Site's 'Average' Supernatant: Distribution Coefficients vs. Time," Oak Ridge National Laboratory, Oak Ridge, TN (1998).

Koh, J.-H., P. C. Wankat, and N.-H. L. Wang, "Pore and Surface Diffusion and Bulk-Phase Mass Transfer in Packed and Fluidized Beds," *Ind. Eng. Chem. Res.*, **37**, 228 (1998).

Lee, D. D., J. F. Walker, Jr., P. A. Taylor, and D. W. Hendrickson, "Cesium-Removal Flow Studies Using Ion Exchange," *Environ. Prog.* **16**, 251 (1997).

Ma, Z., R. D. Whitley, and N.-H. L. Wang, "Pore and Surface Diffusion in Multicomponent Adsorption and Liquid Chromatography Systems," *AIChE J.*, **42**, 1244 (1996).

McCabe, D. J., "Crystalline Silicotitanate Examination Results," Technical Report WSRC-RP-94-1123, Westinghouse Savannah River Company, Aiken, SC (1995).

McCabe, D. J., "Examination of Crystalline Silicotitanate Applicability in Removal of Cesium from SRS High Level Waste," Technical Report WSRC-TR-97-0016, Westinghouse Savannah River Company, Aiken, SC (1997).

McGinnis, C. P., R. D. Hunt, S. M. Gibson, and R. L. Gilchrist, "Separation Projects within the U. S. Department of Energy's Underground Storage Tank—Integrated Demonstration," *Sep. Sci. Tech.*, **30**, 1741 (1995).

Walker, D. D., W. D. King, D. P. Diprete, L. L. Tovo, D. T. Hobbs, and W. L. Wilmarth, "Cesium Removal from Simulated SRS High-Level Waste Using Crystalline Silicotitanate," Technical Report WSRC-TR-98-00344, Rev.1, Westinghouse Savannah River Company, Aiken, SC (1998).

Walker, Jr., J. F., P. A. Taylor, R. L. Cummins, B. S. Evans, S. D. Heath, J. D. Hewitt, R. D. Hunt, H. L. Jennings, J. A. Kilby, D. D. Lee, S. Lewis-Lambert, S. A. Richardson, and R. F. Utrera, "Cesium Removal Demonstration Using Crystalline Silicotitanate Sorbent for Processing Melton Valley Storage Tank Supernate: Final Report," Technical Report ORNL/TM-13503, Oak Ridge National Laboratory, Oak Ridge, TN (1998).

Whitley, R. D., *Dynamics of Nonlinear Multicomponent Chromatography—Interplay of Mass Transfer, Intrinsic Sorption Kinetics, and Reaction*, Ph.D. Thesis, Purdue University, West Lafayette, IN (1990).

Wilson, E. J., and C. J. Geankoplis, "Liquid Mass Transfer at Very Low Reynolds Numbers in Packed Beds," *Ind. Eng. Chem. Fundam.*, **5**, 9 (1966).

Zheng, Z., R. G. Anthony, and J. E. Miller, "Modeling Multicomponent Ion Exchange Equilibrium Utilizing Hydrous Crystalline Silicotitanates by a Multiple Interactive Ion Exchange Site Model," *Ind. Eng. Chem. Res.*, **36**, 2427 (1997).

TABLE I. Dimensionless parameters in the pore diffusion model (Eqs. 3 and 4).

Parameter	Definition	Description	Value†
X	z/L_c	dimensionless axial distance	0-1
θ	tu_0/L_c	dimensionless time	0-1
xi	r/R_p	dimensionless radial distance	0-1
φ_b	$(1-\varepsilon_b)/\varepsilon_b$	particle/bulk phase ratio	1.0
φ_p	$(1-\varepsilon_p)/\varepsilon_p$	solid/pore phase ratio	3.2
L_c^*	L_c/R_p	dimensionless column length	1.8×10^4
k_f^*	k_f/u_0	film mass transfer/convection	3.3×10^{-2}
Pe_b	u_0L_c/E_b	convection/axial dispersion	3.8×10^3
Pe_p	u_0R_p/D_p	convection/intraparticle diffusion	2.5×10^3

†I.D. = 4 ft. L_c = 11.3 ft. u_s = 4.9 cm/min. R_p = 187.5 μm. $D_p = 7.3 \times 10^{-5}$ cm^2/min.

TABLE 2. SRS waste compositions.

	Concentration [mol/L]					
Component	Avg	Avg-b	OH	OH-b	NO_3	NO_3-b
Na^+	5.6	5.47	5.6	5.48	5.6	5.45
K^+	0.015	0.15	0.03	0.15	0.0041	0.15
Cs^+	0.00014	0.0007	0.00037	0.0007	0.00014	0.0007
AlO_2^-	0.31	0.31	0.27	0.27	0.32	0.32
$C_2O_4^{2-}$	0.008	0.008	0.008	0.008	0.008	0.008
CO_3^{2-}	0.16	0.16	0.17	0.17	0.16	0.16
MoO_4^{2-}	0.0002	0.0002	0.0002	0.0002	0.0002	0.0002
SiO_3^{2-}	0.004	0.004	0.004	0.004	0.004	0.004
SO_4^{2-}	0.15	0.15	0.030	0.030	0.22	0.22
PO_4^{3-}	0.010	0.010	0.008	0.008	0.010	0.010
Cl^-	0.025	0.025	0.010	0.010	0.040	0.040
F^-	0.032	0.032	0.010	0.010	0.050	0.050
NO_2^-	0.52	0.52	0.74	0.74	0.37	0.37
NO_3^-	2.14	2.14	1.10	1.10	2.84	2.84
OH^-	1.91	1.91	3.05	3.05	1.17	1.17

TABLE 3. Langmuir coefficients for modeling SRS and ORNL column tests.

Waste	*a* [mL/mL B.V.]	*b* [mL/mg]
SRS average	2400	30.9
SRS average, bounding	1530	19.8
SRS high OH	2900	37.6
SRS high OH, bounding	1960	25.3
SRS high NO_3	2030	26.3
SRS high NO_3, bounding	1280	16.7
MVST-W29	846	11.9

TABLE 4. System and mass transfer parameters used in carousel simulations.

Parameter	Value, 15 gpm	Value, 25 gpm	Source
I. D. [ft]	4.0	4.3	
L_c [ft]	11.3	16.0	
R_p [μm]	187.5	187.5	McCabe (1995)
ε_b [-]	0.50	0.50	Anthony (1998)
ε_p [-]	0.24	0.24	Anthony (1998)
D_{infty} [cm^2/min]	9.4×10^{-4}	9.4×10^{-4}	Ernest et al. (1997)
D_p [cm^2/min]	7.3×10^{-5}	7.3×10^{-5}	Stokes-Einstein
k_f [cm/min]	0.316	0.357	Wilson-Geankoplis(1966)
E_b [cm^2/min]	0.883	1.27	Chung-Wen (1968)

TABLE 5. Case 1. Column length requirement for a fixed column diameter of 4 ft. SRS wastes are as defined in Table 2. The letter b indicates a high K^+ (bounding) case. R_p = 187.5 μm. $D_p = 7.3 \times 10^{-5}$ cm^2/min. L_{MTZ} = single column length in a three column carousel. $L_{tot} = 3 \times L_{MTZ}$. TAMU equilibrium parameters are used without a dilution factor.

SRS waste	Flow rate [gpm]	u_s [cm/min]	u_0 [cm/min]	Pe_p	L_{MTZ} [ft]
Average	15	4.9	9.8	2.50×10^3	11.3
	25	8.1	16.2	4.16×10^3	18.6
Average (b)	15	4.9	9.8	2.50×10^3	5.3
	25	8.1	16.2	4.16×10^3	8.7
High OH	15	4.9	9.8	2.50×10^3	5.1
	25	8.1	16.2	4.16×10^3	8.4
High OH (b)	15	4.9	9.8	2.50×10^3	**4.5**
	25	8.1	16.2	4.16×10^3	7.4
High NO_3	15	4.9	9.8	2.50×10^3	12.8
	25	8.1	16.2	4.16×10^3	**20.9**
High NO_3 (b)	15	4.9	9.8	2.50×10^3	6.0
	25	8.1	16.2	4.16×10^3	9.9

TABLE 6. Case 2. Column diameter requirement for a fixed column-segment length of 16 ft. R_p = 187.5 μm. $D_p = 7.3 \times 10^{-5}$ cm²/min.

SRS waste	Flow rate [gpm]	u_s [cm/min]	u_0 [cm/min]	I.D. [ft]
Average	15	7.0	16.0	3.3
	25	7.0	16.0	4.3
Average (b)	15	14.9	29.8	2.3
	25	14.9	29.8	3.0
High OH	15	15.4	30.8	2.2
	25	15.4	30.8	2.9
High OH (b)	15	17.5	35.0	**2.1**
	25	17.5	35.0	2.7
High NO_3	15	6.2	12.4	3.5
	25	6.2	12.4	**4.6**
High NO_3 (b)	15	13.1	26.2	2.4
	25	13.1	26.2	3.1

TABLE 7. Comparison of two carousel processes operated at two different volumetric flow rates. Isotherm is based on SRS average nominal waste with a dilution factor of 1.0. $D_p = 7.3 \times 10^{-5}$ cm²/min. R_p = 187.5 μm.

Flow rate [gpm]	15	25
I. D. [ft]	4.0	4.3
Interstitial velocity [cm/min]	9.7	16.0
Superficial velocity [cm/min]	4.9	8.0
L_{MTZ} [ft]	11.3	16.0
Total bed volume [ft³]	426	697
Percent column saturation	99	99
Switch time [days]	74	73

TABLE 8. Comparison of carousel configurations with varying numbers of segments. Column cross-sectional area and flow rates are fixed.

Number of segments	Total bed length	Relative TPBV	Guard column length	Number of valves
3	$3L_{MTZ}$	1	L_{MTZ}	3
4	$2L_{MTZ}$	1.5	$0.50L_{MTZ}$	4
5	$1.67L_{MTZ}$	1.8	$0.33L_{MTZ}$	5
6	$1.5L_{MTZ}$	2.0	$0.25L_{MTZ}$	6

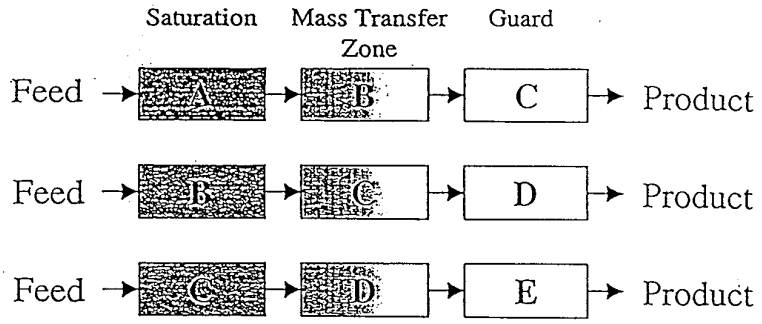

Figure 1. Proposed carousel process. Column 1 is the saturation zone. Column 2 contains the mass transfer zone. Column 3 is a guard zone.

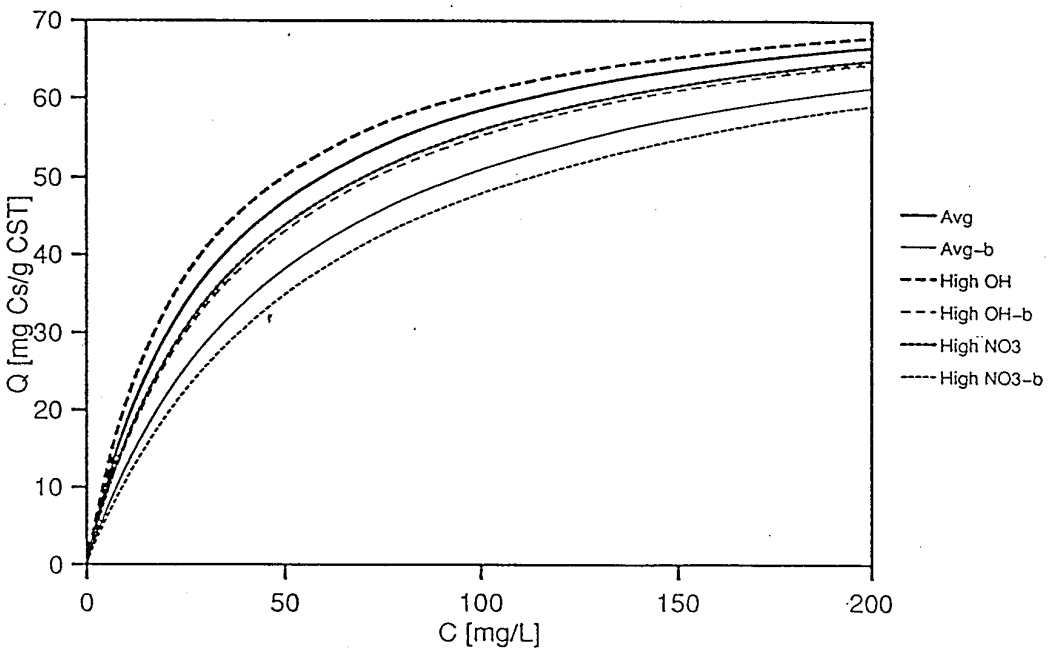

Figure 2. Cs^+/CST isotherms showing model predictions of bounding cases: average SRS, high hydroxide, and high nitrate. Experimental data are shown in symbols.

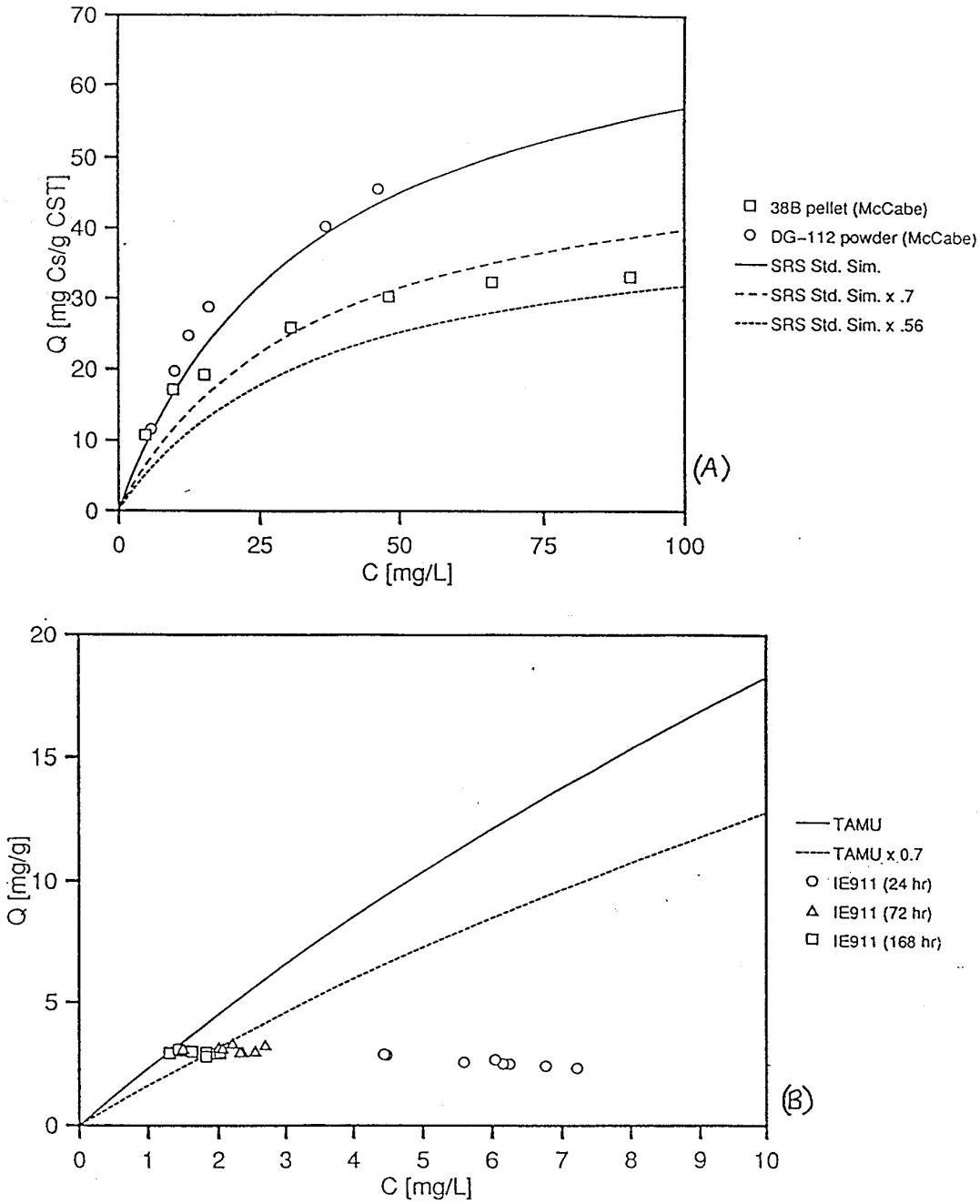

Figure 3. (a) Cs^+/CST isotherms in SRS high level waste. Solid line: TAMU prediction for powdered CST Circles: experimental batch Cs^+ uptake on powdered CST. Triangles: batch data on 38B. Dashed lines: TAMU model prediction multiplied by 0.56 and 0.7. (b) Cs^+/CST isotherms in SRS average waste. Symbols denote batch samples at 24, 72, and 168 hours.

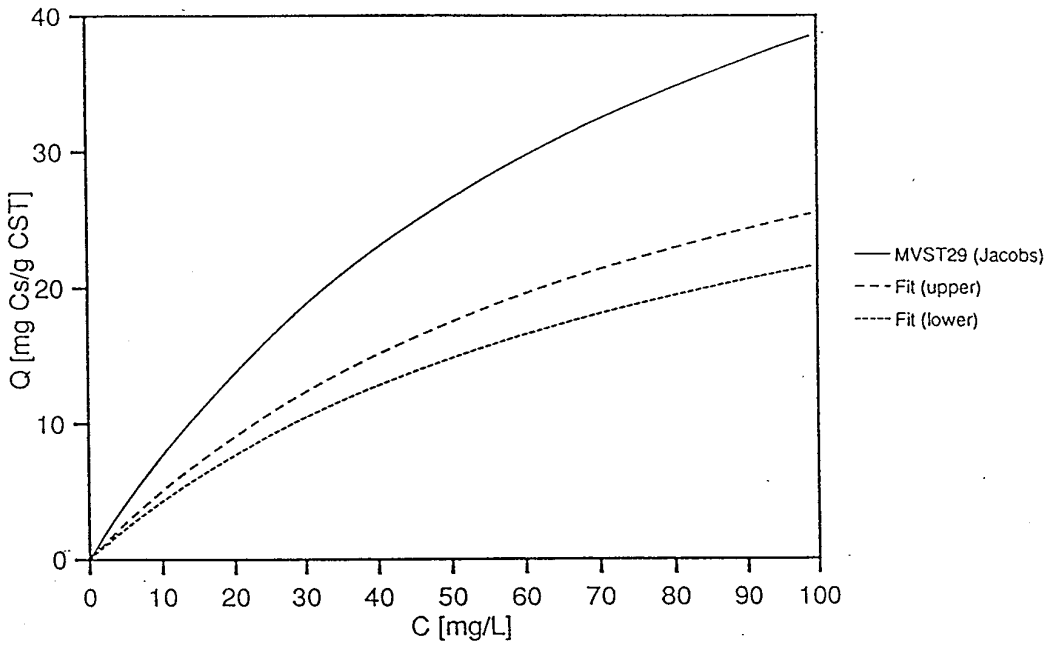

Figure 4. Cs^+/CST isotherm. The solid line denotes the TAMU model of Cs^+ uptake on powdered CST in MVST-29 waste. The dashed lines represent the upper and lower bounds of isotherms that predict column data on engineered CST in MVST-29 waste.

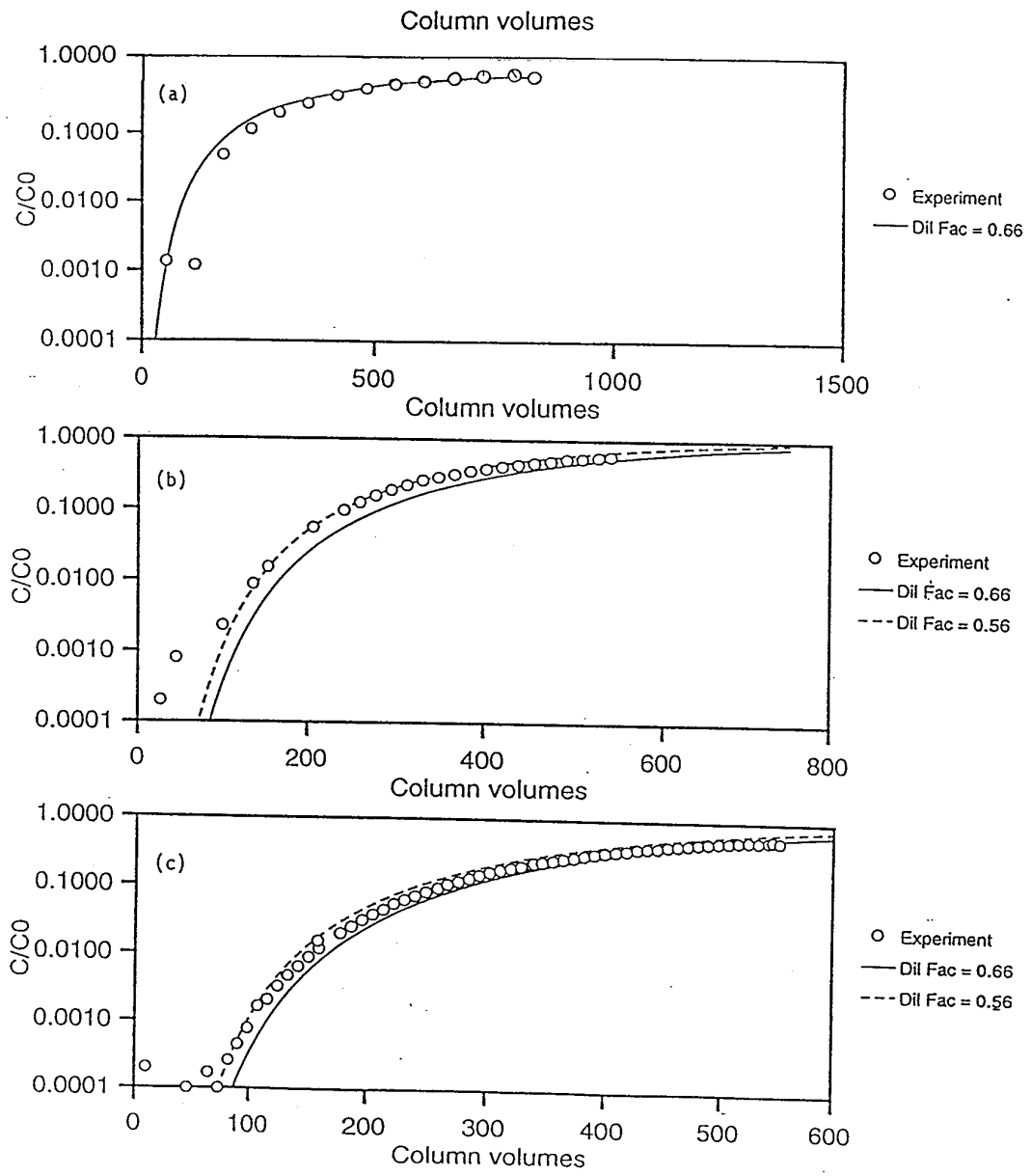

Figure 5. CsRD support column experiments compared to simulation. $D_p = 1.0 \times 10^{-4}$ cm^2/min. (a) $V_c = 10.0$ mL; I. D. = 1.45 cm; $F = 1.00$ mL/min. (b) $V_c = 12.54$ mL; I. D. = 1.45 cm; $F = 0.627$ mL/min. (c) $V_c = 23.2$ mL total; I. D. = 1.45 cm; $F = 1.16$ mL/min.}

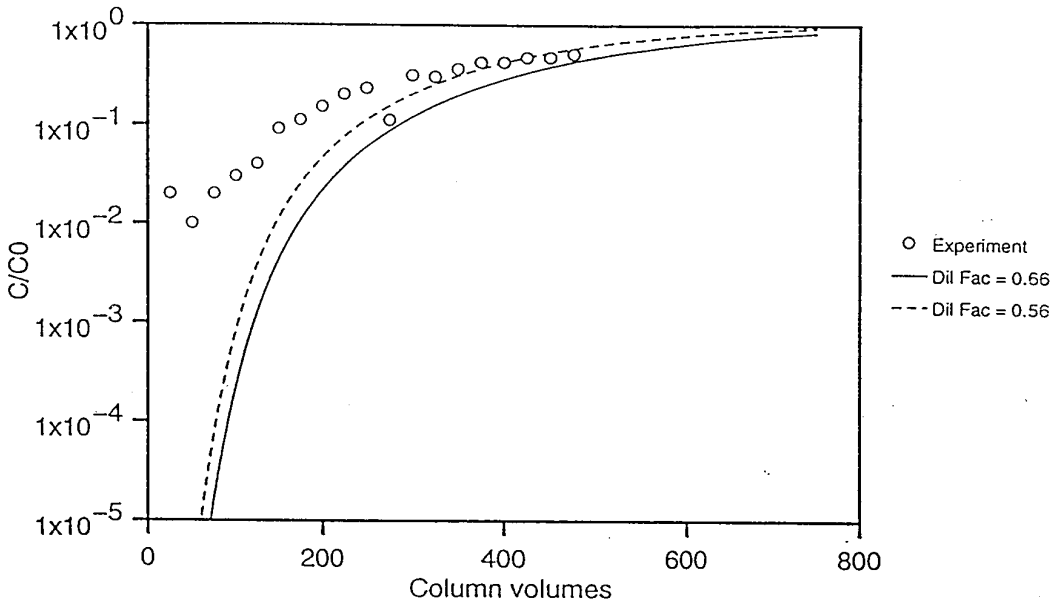

Figure 6. CsRD column experiment compared to simulation. Isotherms are estimated by multiplying TAMU model prediction by 0.56 and 0.66. Column volume: 38 L. Column diameter: 30 cm. Flow rate: 1.9 L/min. $D_p = 1.0 \times 10^{-4}$ cm^2/min.

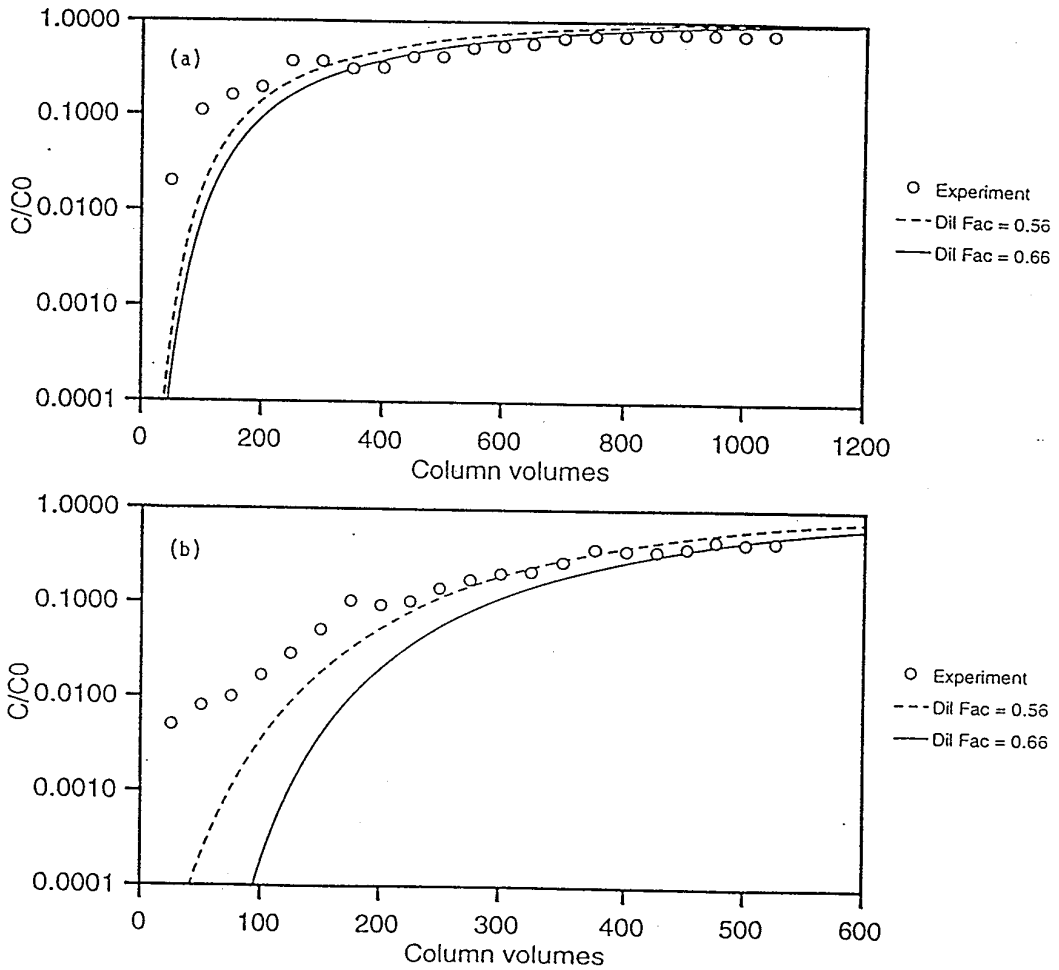

Figure 7. CsRD two-column experiment compared to simulation. Isotherm is estimated by multiplying TAMU model prediction by 0.56 and 0.66. (a) Lead column effluent history. (b) Second column effluent history. Column volume: 38 L (each column). Column diameter: 30 cm. Flow rate: 3.8 L/min. $D_p = 1.0 \times 10^{-4}$ cm^2/min.

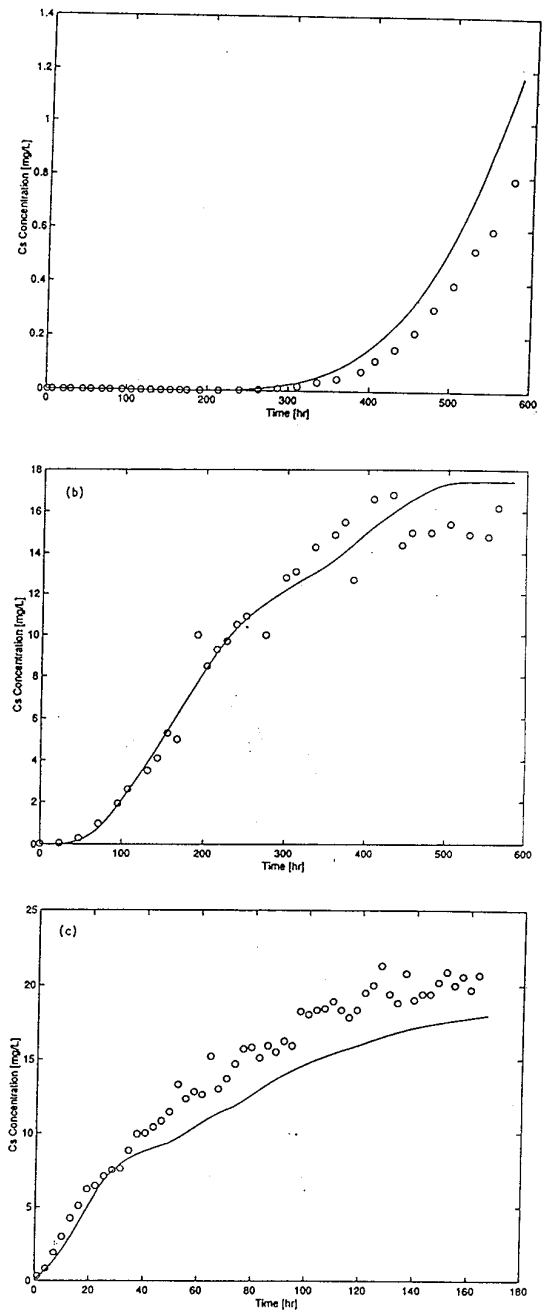

Figure 8. WSRC column experiments compared to simulation. The isotherm parameters are from the TAMU model, without a dilution factor. Column volume: 17.7 mL. (a) $u_s = 0.27$ cm/min. (b) $u_s = 0.98$ cm/min. (c) $u_s = 4.1$ cm/min.

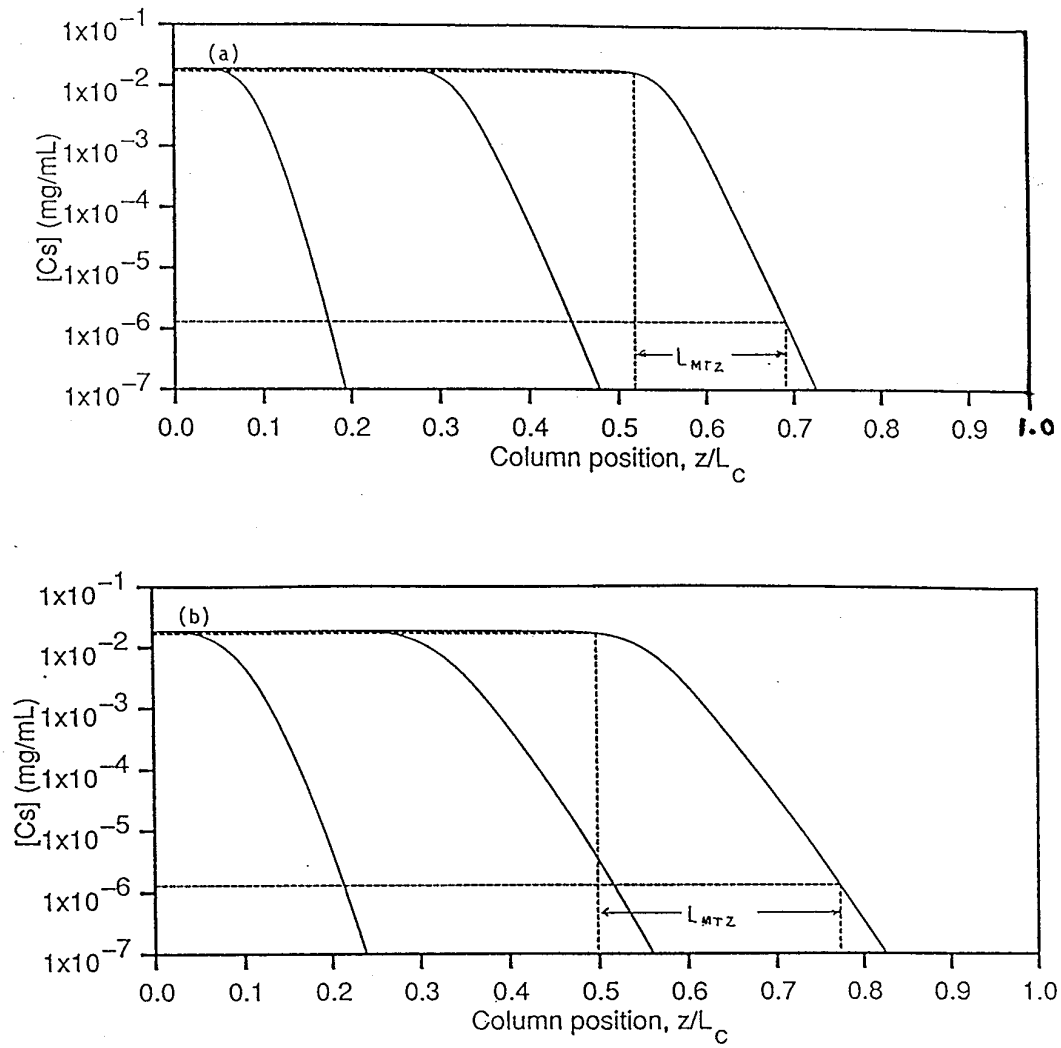

Figure 9. Mass transfer zone length determination for cesium in average SRS waste (nominal). Column diameter: 4 ft. Column length: 66 ft. Dilution factor: 0.7. L_{MTZ} determined from the profile where the concentration decreases from $C/C_0 = 0.9$ to $C = 1.3 \times 10^{-3}$ mg/L. (a) F = 15 gpm. u_s = 4.9 cm/min. (b) F = 25 gpm. u_s = 8.1 cm/min.

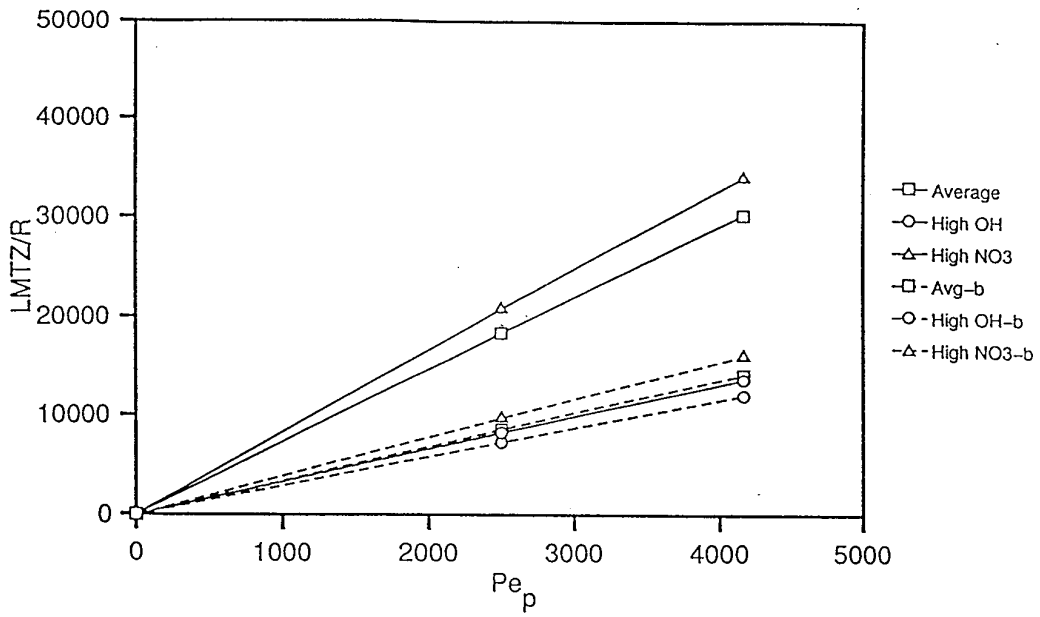

Figure 10. Dimensionless mass transfer zone length as a function of the Peclet number.

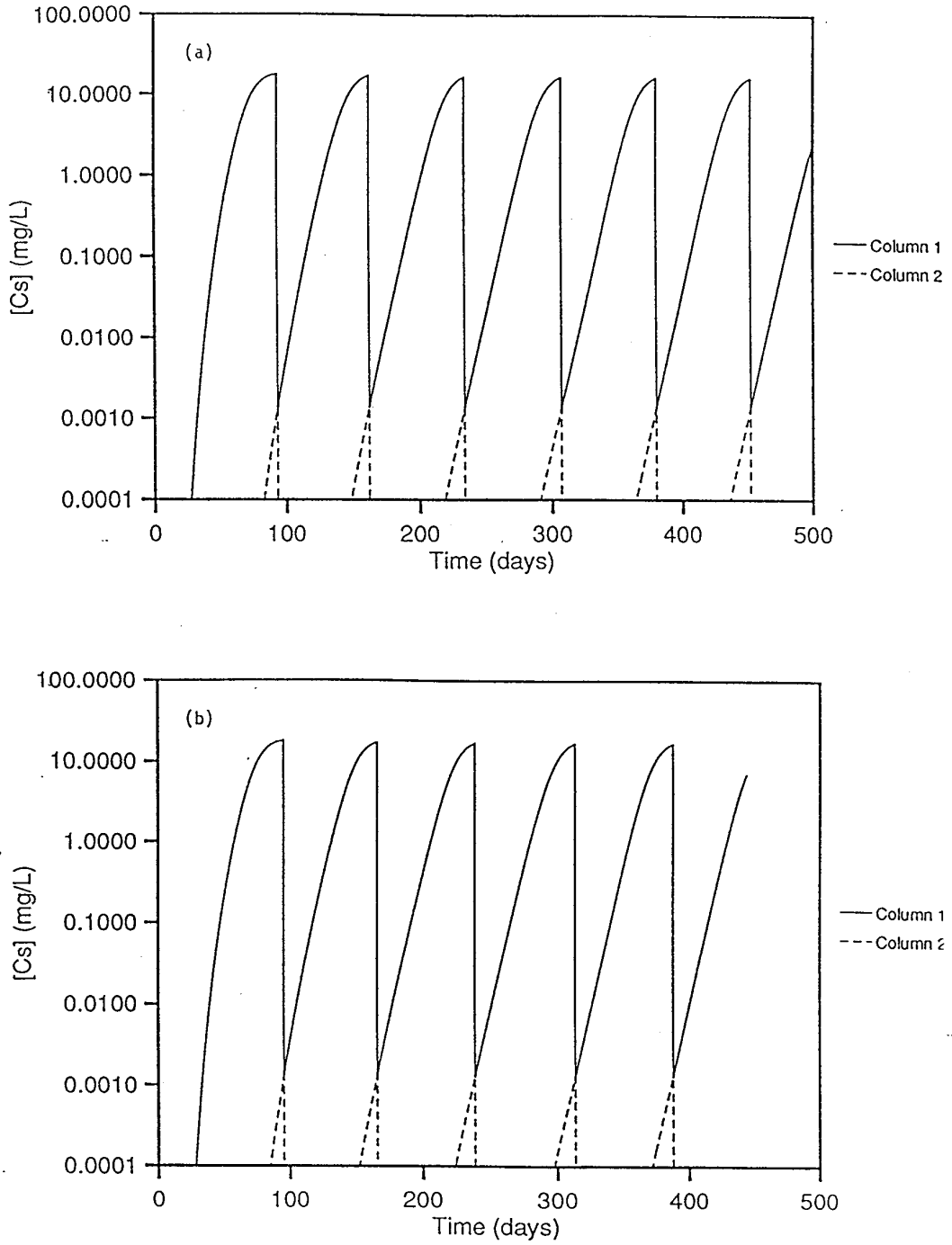

Figure 11. Simulated Cs^+ concentration histories at each outlet port in a three-column carousel process. Feed: average SRS. $D_p = 7.3 \times 10^{-5}$ cm^2/min. Saturation of lead column: 99 percent. Solid line: lead column history. Dashed line: second column history. The outlet concentration of the third column is below 10^{-7} mg/mL. (a) Total bed length: 33.9 ft. Flow rate: 15 gpm. (b) Total bed length: 48.0 ft. Flow rate: 25 gpm.